








Comparison of Single- and Multi-Echo Susceptibility-Weighted Imaging in Detecting Cerebral Arteriovenous Shunts: A Preliminary Study


뇌동정맥단락 진단에서의 단일 에코 자화율 강조영상과 다중 에코 자화율 강조영상의 비교: 예비 연구

Seung Wan Han, MD¹ , Jae Ho Shin, MD^{1*} , Yon Kwon Ihn, MD¹ ,
Seung Ho Yang, MD² , Jae Hoon Sung, MD² 


Departments of ¹Radiology and ²Neurosurgery, St. Vincent's Hospital, The Catholic University of Korea, Suwon, Korea

ORCID iDs

Seung Wan Han  <https://orcid.org/0000-0001-5704-5507>

Jae Ho Shin  <https://orcid.org/0000-0001-5922-5720>

Yon Kwon Ihn  <https://orcid.org/0000-0002-3770-308X>

Seung Ho Yang  <https://orcid.org/0000-0002-3490-1064>

Jae Hoon Sung  <https://orcid.org/0000-0003-3738-6413>

Received May 30, 2022

Revised July 13, 2022

Accepted July 28, 2022

*Corresponding author

Jae Ho Shin, MD

Department of Radiology,

St. Vincent's Hospital,

The Catholic University of Korea,

93 Jungbu-daero, Paldal-gu,

Suwon 16247, Korea.

Tel 82-31-249-7492

Fax 82-31-1577-8588

E-mail shinjh@catholic.ac.kr

This is an Open Access article distributed under the terms of the Creative Commons Attribution Non-Commercial License (<https://creativecommons.org/licenses/by-nc/4.0/>) which permits unrestricted non-commercial use, distribution, and reproduction in any medium, provided the original work is properly cited.

Purpose To compare the sensitivities of T2-weighted image (T2WI) and susceptibility-weighted imaging (SWI) in detecting cerebral arteriovenous fistula (AVF), cerebral arteriovenous malformation (AVM), and carotid-cavernous sinus fistula (CCF), and to qualitatively evaluate single-echo SWI (s-SWI) and multi-echo SWI (m-SWI) in characterizing vascular lesions.

Materials and Methods From January 2016 to December 2021, cerebral angiography-proven lesions were recruited. The sensitivities of T2WI and SWI in detecting vascular lesions were compared using McNemar's test. Qualitative evaluations of s-SWI and m-SWI were categorized to be of poor, average, or good quality and compared using Fisher's exact test.

Results A total of 24 patients (mean age: 61 years, 12 female, and 12 male) were enrolled. Twenty patients underwent s-SWI or m-SWI, and four patients underwent both. AVF, AVM, and CCF were diagnosed in 10, 11, and 3 patients, respectively. SWI demonstrated higher sensitivity compared to that of T2WI (82.1% vs. 53.6%, $p = 0.013$). m-SWI showed better image quality compared to that of s-SWI (good quality, 83.3% vs. 25.0%, $p = 0.009$).

Conclusion SWI demonstrated a higher sensitivity for detecting cerebral arteriovenous shunts com-

pared to that of T2WI. m-SWI exhibited better image quality compared to that of s-SWI in characterizing vascular lesions.

Index terms Magnetic Resonance Imaging; Arteriovenous Fistula; Arteriovenous Malformation; Carotid-Cavernous Sinus Fistula; Angiography

INTRODUCTION

The incidence of cerebral arteriovenous shunts, such as arteriovenous fistula (AVF), arteriovenous malformation (AVM), carotid-cavernous sinus fistula (CCF) is low. Studies have reported that AVF accounts for 10%–15% of intracranial vascular malformations; the incidence of AVM is 1.12–1.42 cases per 100000 person-year; and traumatic CCF accounts for 0.2% of cerebral traumas (1-4). Rupture and hemorrhage may occur, depending on the extent and pathophysiology of vascular lesions, and lead to serious neurological complications (2, 5-7). Furthermore, initial presenting symptoms may vary, and diagnosis can be difficult, although some ocular symptoms (chemosis and ocular pain) are related to CCF (4, 8).

Various imaging modalities are used to evaluate cerebral arteriovenous shunts; namely, non-invasive contrast-enhanced MR angiography (MRA) and relatively invasive transfemoral cerebral angiography (TFCA). The most accurate modality for detecting, characterizing, and obtaining relevant information for clinical grading is TFCA because it depicts hemodynamics and extent of vascular lesions. Nevertheless, given the low prevalence of cerebral arteriovenous shunts, MRA and TFCA may not be applicable to all patients. Instead, efficient, and non-contrast enhanced MR sequences such as T2-weighted image (T2WI), susceptibility weighted images (SWIs), and time-of-flight (TOF) angiography are performed.

Conventional T2WI has MR features of flow-voids in the vicinity of the nidus, thus yielding good diagnostic performance in detecting AVMs larger than 3 cm (9, 10). Similarly, cerebral AVF has T2WI findings of conglomerated dilated leptomeningeal veins, represented by clusters of flow voids. In severe cases of venous congestion caused by an AVF, increased T2WI signals in the adjacent brain parenchyma may be present (11). Several studies have evaluated the diagnostic performance of different MR protocols in the detection of cerebral arteriovenous shunts, of which SWI demonstrated promise for efficiency, good spatial resolution, and the convenience of not requiring contrast media (12-15). Moreover, SWI indirectly provides information regarding levels of oxygenated hemoglobin in the vessels (16).

The development of multi-echo SWI (m-SWI) has enabled better resolution and visualization of small cerebral veins than conventional TOF angiography and single-echo SWI (s-SWI) (17, 18). However, no studies have directly compared s-SWI and m-SWI in terms of detecting and characterizing cerebral arteriovenous shunts. The present study aimed to compare the sensitivity of T2WI and SWI for detecting cerebral arteriovenous shunts (AVF, AVM, CCF), and to qualitatively evaluate s-SWI and m-SWI in characterizing vascular lesions.

MATERIALS AND METHODS

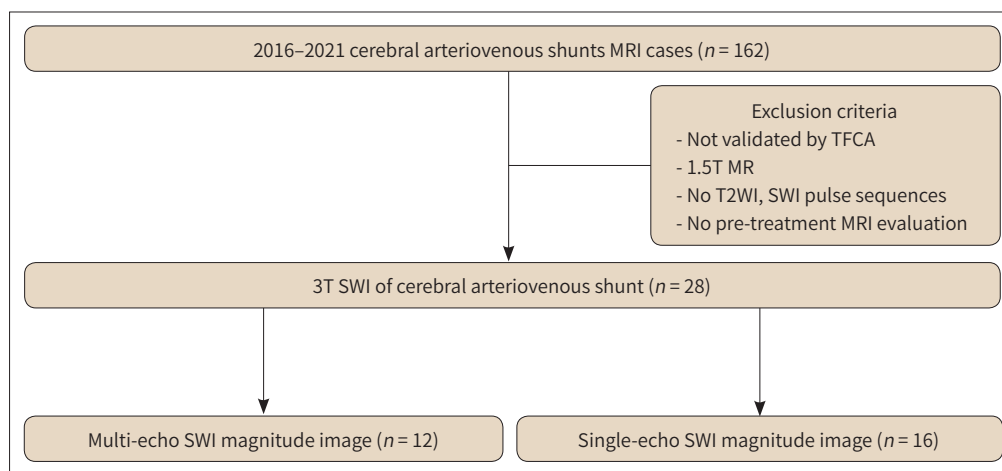
This single-center retrospective study, medical image reviews (MRI, TFCA), and medical record reviews were approved by the Institutional Review Board (IRB No. VC22RASI0052), and requirements for consent forms were waived. Patients with suspected AVF, AVM or CCF on MRI between January 2016 to December 2021 were initially recruited. All patients underwent TFCA within 12 months acquisition of MRI. Specifically, the median time interval between MRI acquisition and TFCA was approximately 8.5 days with interquartile range of 2.0 days to 22.3 days. However, individuals who did not undergo TFCA or TFCA within 12 months of MRI acquisition, those who underwent 1.5T MRI, MRI without T2WI or SWI pulse sequences, and individuals without pre-treatment MRI SWI evaluation were excluded (Fig. 1). Three MR vendors utilized in present study were the Vida 3T MRI (Siemens, Erlangen, Germany), Ingenia 3T MRI (Phillips, Cambridge, MA, USA), and Verio 3T MRI (Siemens).

MR PROTOCOL

All MR pulse sequences in our study (T2WI, SWI) were scanned from foramen magnum to calvaria vertex level, and all pulse sequences utilized a single number of excitation. The slice thickness of T2WI and SWI were 5 mm and 2 mm, respectively. The following MR parameters were utilized for T2WI: (echo time [TE]: Ingenia: 80 ms, Verio: TE: 95 ms, Vida TE: 88 ms; repetition time [TR]: Ingenia: 3000 ms, Verio: 4890 ms, Vida: 4200 ms; field of view [FOV]: Ingenia: 220 × 220; Verio: 230 × 230; Vida: 220 × 220; acquisition matrix: Ingenia: 512 × 354, Verio: 230 × 230; Vida: 220 × 220).

The m-SWI images were obtained using Ingenia 3T MRI with total image acquisition time of 130 seconds. The parameters for m-SWI were as follow: (TE: 7.2 ms–13.5 ms–19.8 ms–26.0 ms; TR: 31 ms; flip angle [FA]: 17°; acquisition matrix: 368 × 368; FOV: 220 × 220) The s-SWI images

Fig. 1. Study design.



TFCA-proven cerebral arteriovenous shunts from January 2016 to December 2021 were included in the study. Exclusion criteria were lack of validation by TFCA, 1.5T MRI, no T2WI, no SWI pulse sequences, and unavailability of pretreatment MRI.

SWI = susceptibility weighted image, TFCA = transfemoral cerebral angiography, T2WI = T2-weighted image

were obtained using either Verio 3T MRI or Vida 3T MRI. The image acquisition time for s-SWI was 181 seconds for Verio 3T MRI and 182 seconds for Vida 3T MRI. The parameters for s-SWI were as follow: Verio: (TE: 20 ms; TR: 28 ms; FA: 15°; acquisition matrix: 384 × 278; FOV: 208 × 230), Vida: (TE: 19.6 ms; TR: 26 ms; FA: 17°; acquisition matrix: 512 × 307; FOV: 220 × 220).

TFCA PROTOCOL

Vascular lesions were validated by the TFCA. The right femoral artery was accessed for control angiography, using a bi-plane angiography device (Artis Zee RF-1000-125 Biplane, Siemens). Selection of bilateral internal carotid artery, external carotid artery, and vertebral arteries were performed with 5F-diagnostic catheters. Digital subtraction angiography (DSA) was performed with frontal and lateral projection rate of 2 frames per second. If abnormal vessels (early draining veins or nidus) were visualized on angiography, specific feeding vessels were selected, and three-dimensional DSAs were performed to evaluate feeders, draining veins, and extent of the vascular lesions. For the TFCA analysis, the Borden classification was used for AVF, Spetzler-Martin grade for AVM, and Barrow classification for CCF (3, 8, 19, 20).

IMAGE ANALYSIS: T2WI, SWI

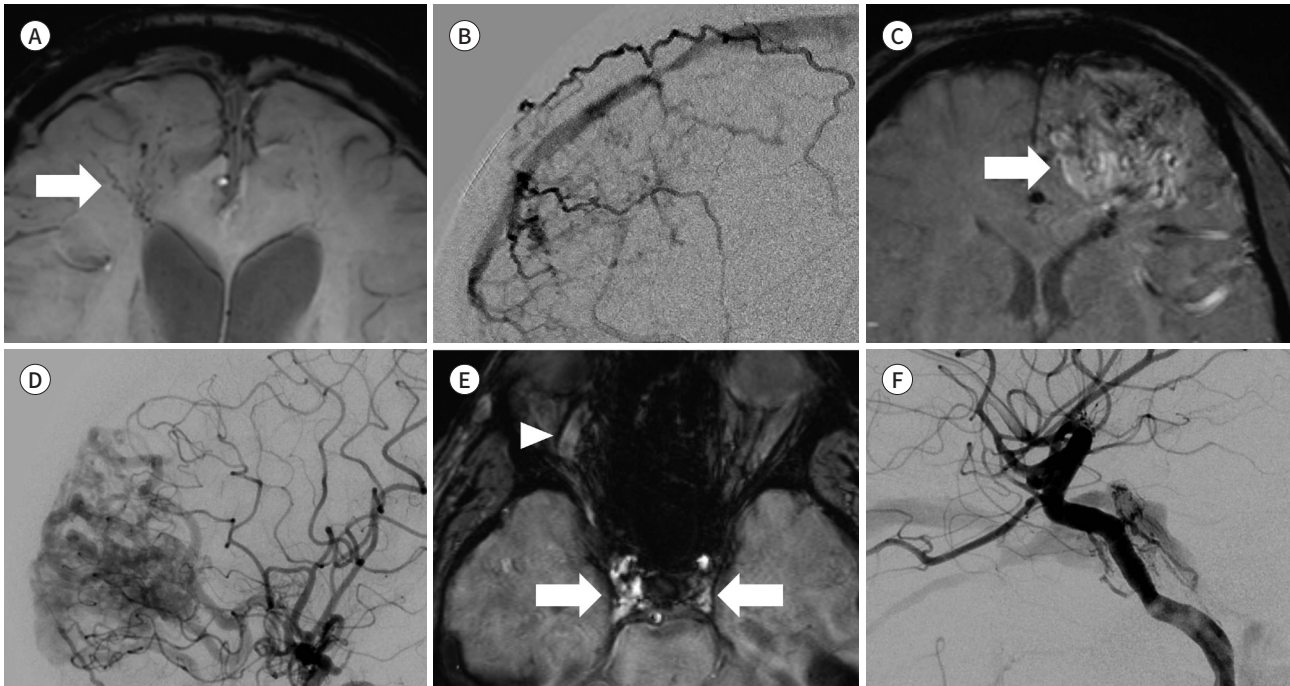
After blinding of the TFCA findings, clinical information, and final diagnosis, two readers (one neuroradiologist and one neurosurgeon) independently evaluated T2WI, s-SWI magnitude images, m-SWI magnitude images, and disagreements were resolved by consensus. For T2WI, localized, conglomeration of flow-voids was a positive finding of AVM nidus, while regionally distributed clusters of flow-voids, and increased T2WI signals in the adjacent brain parenchyma were findings of AVF. Any subtle increase in T2WI signals and asymmetric vessels were negative findings because small vessel disease, encephalomalacia, and vascular variants (prominent pial vessels) may mimic AVF findings. For CCF, visualization of superior ophthalmic vein dilatation, asymmetric distension of cavernous sinus, and proptosis of the orbits were considered positive findings (21).

The following SWI findings were positive for AVF on magnitude image: regionally distributed dilated small veins (pseudophlebitic pattern); abnormally increased signals within cerebral sinuses and cerebral veins; and asymmetrically distended veins or venous aneurysmal change (22). Any subtle findings, such as scattered dark signals and localized small vessels, were negative findings for AVF because non-specific parenchymal calcifications or microbleeding may mimic AVF. For AVM, localized and conglomeration of vessels with heterogeneous signals were considered positive findings. For CCF, increased signals in the distended superior ophthalmic vein and cavernous sinus were considered positive findings (Fig. 2).

Image qualities of both s-SWI and m-SWI magnitude images were qualitatively evaluated and categorized as poor, average, and good quality. Vascular lesions that were difficult to visualize and difficult to evaluate extent of the lesion were considered poor quality. Vascular lesions suspected on SWI with limited evaluation of AVM nidus size, AVF extent, possible feeders, and draining veins were considered average quality. Finally, visualization of vascular lesions with approximation of AVM nidus, AVF extent, possible feeders, and draining veins were considered good quality.

Fig. 2. Features of SWI magnitude image of cerebral arteriovenous shunts.

A-F. SWI (**A, C, E**), TFCA (**B, D, F**). Representative cerebral arteriovenous shunt cases in SWI (**A-C**) validated using TFCA (**D-F**). (**A**) m-SWI demonstrates regional tortuous dilatation (arrow) of small veins, considered to be pseudophlebitic signs of an AVF. (**B**) TFCA demonstrates AVF with feeders from the bilateral middle meningeal arteries and distal branches of ACA. (**C**) s-SWI demonstrates a large AVM in the left frontal lobe with conglomeration of vessels and heterogeneous signals (arrow). (**D**) TFCA demonstrates AVM with multiple feeders from the ACA A1, left ACA A2, and left MCA. (**E**) s-SWI demonstrates bilateral CCF with increased signals at both the cavernous sinuses (arrows) and the distended right superior ophthalmic vein (arrowhead). (**F**) Selective angiography of the right internal carotid demonstrates CCF Barrow classification D draining into the ipsilateral superior ophthalmic vein and inferior petrosal sinus. ACA = anterior cerebral artery, AVF = arteriovenous fistula, AVM = arteriovenous malformation, CCF = carotid-cavernous sinus fistula, MCA = middle cerebral artery, m-SWI = multi-echo SWI, s-SWI = single-echo SWI, SWI = susceptibility weighted image, TFCA = transfemoral cerebral angiography



STATISTICAL ANALYSIS

All statistical processing of demographic information, sensitivity, image quality, and interobserver agreement were performed with R package (v. 3.6.1, The R Foundation for Statistical Computing). McNemar's test was used to compare sensitivity between T2WI and SWI in detecting cerebral arteriovenous shunts. The image qualities of both SWI modalities were compared using the Fisher's exact test. The unweighted Cohen's Kappa was calculated for sensitivity evaluation, while the linearly weighted Cohen's Kappa was calculated for image quality evaluation. The following Cohen's Kappa interpretations were used: slight agreement (κ : 0.01–0.20), fair agreement (κ : 0.21–0.40), moderate agreement (κ : 0.41–0.60), substantial agreement (κ : 0.61–0.80), and almost perfect agreement (κ : 0.81–0.99) (23). Differences with a two-sided $p < 0.05$ were statistically significant.

RESULTS

A total of 162 cases with suspected cerebral arteriovenous shunts were recruited. After ap-

Table 1. Demographics of the Patients

	Total Patients (n = 24)
Age, median (IQR)	61 (48, 70)
Sex (female)	12 (50)
SWI modality	
Either single-echo or multi-echo	20 (83.3)
Both single-echo and multi-echo	4 (16.7)
Initial symptoms	
Asymptomatic	3 (12.5)
Disorientation	3 (12.5)
Headache	6 (25.0)
Motor weakness	3 (12.5)
Ocular symptoms	3 (12.5)
Seizure	3 (12.5)
Others*	3 (12.5)
Cerebral angiography diagnosis	
Arteriovenous malformation	11/24 (45.8)
Spetzler-Martin grade 2	7/11 (63.6)
Spetzler-Martin grade 3	4/11 (36.4)
Arteriovenous fistula	10/24 (41.7)
Borden classification 1	3/10 (30)
Borden classification 2	1/10 (10)
Borden classification 3	6/10 (60)
Cavernous carotid fistula	3/24 (12.5)
Barrow classification A + C	1/3 (33.3)
Barrow classification C	1/3 (33.3)
Barrow classification D	1/3 (33.3)
Rupture/hemorrhage	7 (29.2)
Treatment	
Endovascular	8 (33.3)
Surgery	5 (20.8)
Observation or follow-up loss	11 (45.8)

Data are number of cases with percentages in parentheses.

*Other symptoms include memory impairment, dizziness and syncope.

IQR = interquartile range, SWI = susceptibility weighted image

plying the exclusion criteria, 28 cases among 24 patients (median age, 61 years [interquartile range, 48–70 years]; female: 12/24, [50%]) with TFCA-confirmed cerebral arteriovenous shunts were included in the study (Table 1). Twenty patients underwent either s-SWI or m-SWI, while 4 patients underwent both s-echo and m-SWI, thereby corresponding to a total of 28 SWI acquisitions per 24 patients: 11/24 (45.8%) AVM, 10/24 (41.7%) AVF, 3/24 (12.5%) CCF. Among initial presentations, headache was the most common symptom, 6/24 (25.0%), followed by 3/24 (12.5%) disorientation, 3/24 (12.5%) motor weakness, 3/24 (12.5%) seizure, and 3/24 (12.5%) other symptoms such as acute memory impairment, dizziness, and syncope. Three of 24 (12.5%) patients were asymptomatic. All 3 CCF patients exhibited ocular symptoms, such as chemosis

and/or ocular pain. In the initial MR evaluation, 7/24 (29.2%) patients had intracranial hemorrhages in the form of microbleeding, gross intraparenchymal hemorrhage, and intraventricular hemorrhage.

For AVM, 7/11 (63.6%) patients were categorized as Spetzler-Martin grade 2, while 4/11 (36.4%) were Spetzler-Martin grade 3. For AVF, 3/10 (30%) patients were categorized as Borden classification 1, 1/10 (10%) patients as Borden classification 2, and 6/10 (60%) as Borden classification 3. For CCF, 1/3 (33.3%) patient was categorized as combined Barrow classification A + C, 1/3 (33.3%) as Barrow classification C, and 1/3 (33.3%) as Barrow classification D. Surgery was performed in 5/24 (20.8%) patients, while endovascular treatments were performed in

Table 2. Detection of Cerebral Arteriovenous Shunting on T2WI and SWI

	Sensitivity (%)	95% CI	p-Value
All SWI vs. T2WI (n = 28)			
All SWI	82.1	63.1–93.9	0.013
T2WI	53.6	33.9–72.5	
s-SWI vs. T2WI (n = 16)			
s-SWI	75.0	47.6–92.7	0.134
T2WI	50.0	24.7–75.4	
m-SWI vs. T2WI (n = 12)			
m-SWI	91.7	61.5–99.8	0.134
T2WI	58.3	27.7–84.8	

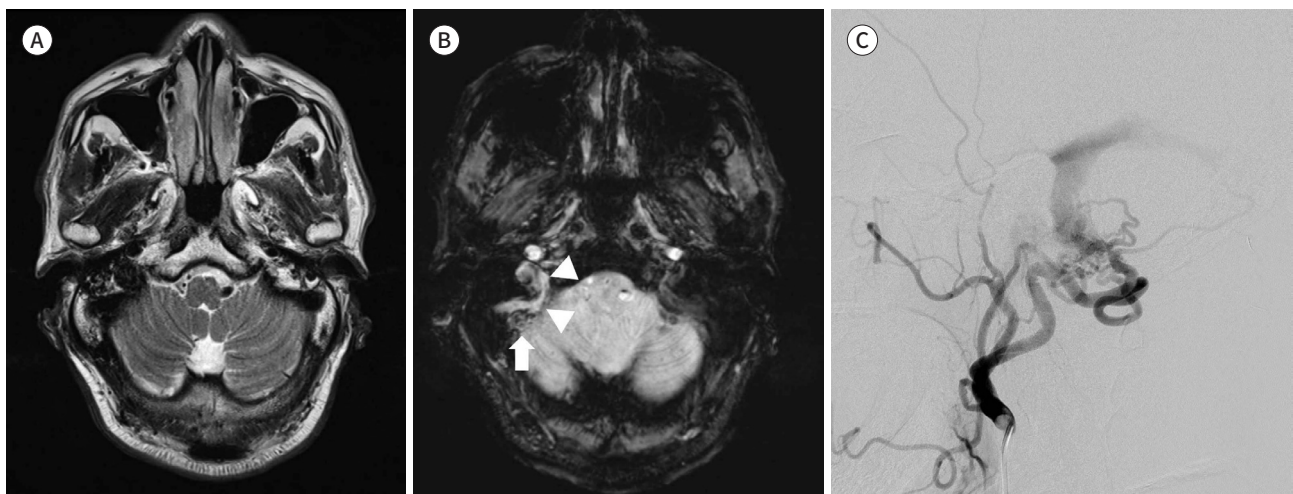
Sensitivity comparison between conventional T2WI and SWI was performed using the McNemar's test with *p* value less than 0.05 as statistically significant.

CI = confidence interval, m-SWI = multi-echo SWI, SWI = susceptibility weighted image, s-SWI = single-echo SWI, T2WI = T2-weighted image

Fig. 3. Cerebral AVF detected by SWI magnitude image.

A-C. A 69-year-old male underwent **(A)** T2WI, **(B)** single-echo SWI, and **(C)** TFCA because of dizziness. **(A)** T2WI shows no AVF, while **(B)** single-echo SWI (average image quality) shows asymmetric distension and increased signals in the right sigmoid sinus (arrowheads) and suspicious dilated vessels in the right cerebellum (arrow). **(C)** Selective angiography of the right external carotid artery demonstrates Borden grade 1 AVF, with feeders from the right occipital artery draining directly into the ipsilateral sigmoid sinus.

AVF = arteriovenous fistula, SWI = susceptibility-weighted image, TFCA = transfemoral cerebral angiography, T2WI = T2-weighted image



8/24 (33.3%). Eleven of 24 (45.8%) patients were under close observation category or follow-up loss category.

In terms of cerebral arteriovenous shunt detection, SWI demonstrated higher sensitivity than T2WI: {82.1% (95% confidence interval [CI]: 63.1–93.9) vs. 53.6% [95% CI: 33.9–72.5], $p = 0.013$ }. However, the sensitivity of each SWI modality was comparable to T2WI: (s-SWI: 75.0% [95% CI: 47.6–92.7] vs. 50.0% [95% CI: 24.7–75.4], $p = 0.134$; m-SWI: 91.7% [95% CI: 61.5–99.8] vs. 58.3% [95% CI: 27.7–84.8], $p = 0.134$) (Table 2). For each specific cerebral arteriovenous shunt, both T2WI and SWI demonstrated comparable sensitivities: AVF: (T2WI: 53.9% [95% CI: 25.1–80.8] vs. SWI: 76.9% [95% CI: 46.2–95.0], $p = 0.371$); AVM: (T2WI: 66.7% [95% CI: 34.9–90.1] vs. SWI: 100% [95% CI: 73.5 vs. 100.0], $p = 0.134$); CCF: (T2WI: 0% vs. SWI: 33.3%, $p = NA$). T2WI performed poorly for detecting AVF due to poor visualization of dilated vessels and lack of flow-related enhancement (Fig. 3). However, T2WI relatively performed better in the

Table 3. Evaluation of Image Quality of Single- and Multi-Echo SWI

Qualitative Evaluation	Total (n = 28)	s-SWI (n = 16)	m-SWI (n = 12)	p- Value
Poor - Difficult visualization of vascular lesion and difficult evaluation of the vascular lesion’s extent	5 (17.9)	4 (25.0)	1 (8.3)	0.009
Average - Suspicious of vascular lesion with limited evaluation of vascular lesion’s extent, venous strain, and nidus	9 (32.1)	8 (50.0)	1 (8.3)	
Good - Visualization of the vascular lesion, and approximation of lesion’s extent	14 (50.0)	4 (25.0)	10 (83.3)	

Data are number of cases with percentages in parentheses. The qualitative evaluations of SWI modalities were categorized into poor, average, and good quality, and comparisons were made by Fisher’s exact test with p value less than 0.05 as statistically significant.

m-SWI = multi-echo SWI, s-SWI = single-echo SWI, SWI = susceptibility weighted image

Fig. 4. Image-quality comparison of single- and multi-echo SWI in detecting cerebral AVM.

A-C. A 72-year-old female underwent (A) s-SWI, (B) m-SWI, and (C) TFCA because of motor weakness. (A) The s-SWI, classified as having average image quality, demonstrates slightly increased signals (arrow) in the left parietal and occipital lobes. (B) The m-SWI, classified as having good image quality, demonstrates much more conspicuous conglomeration of vessels with heterogeneous signals (arrow), suggestive of AVM. (C) TFCA confirms the 2.6 cm-AVM nidus (arrow), with main feeders from the left middle cerebral artery M4 draining into the cortical vein and vein of Trolard.

AVM = arteriovenous malformation, m-SWI = multi-echo SWI, s-SWI = single-echo SWI, SWI = susceptibility-weighted image, TFCA = transfemoral cerebral angiography

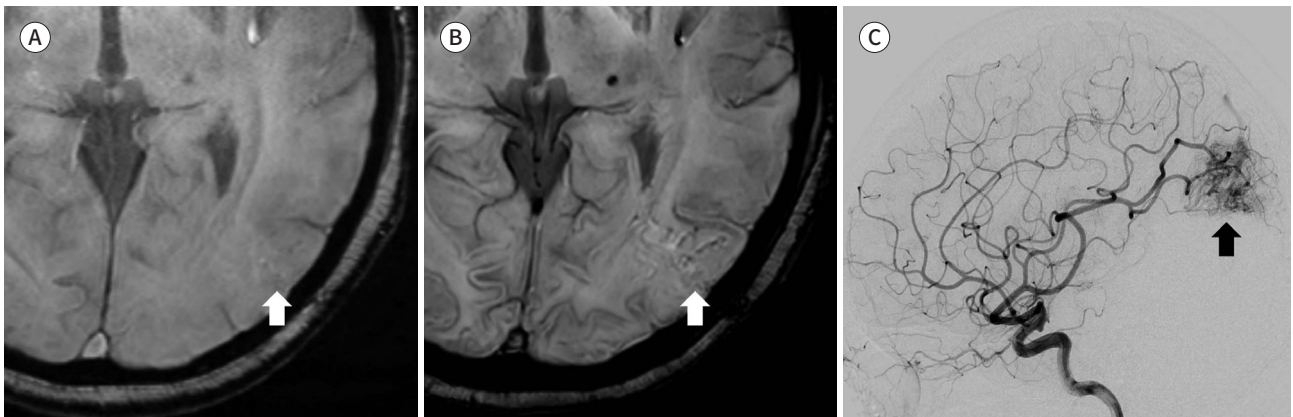


Fig. 5. Comparison of image-quality of single- and multi-echo SWI in detecting cerebral AVF.

A-C. A 67-year-old male underwent **(A)** s-SWI, **(B)** m-SWI, and **(C)** TFCA because of headache. **(A)** The s-SWI, classified as having average image quality, demonstrates subtly dilated veins in the left temporal lobe (arrows). **(B)** The m-SWI, classified as having good image quality, demonstrates a much more conspicuous manifestation of regional dilatation of small veins (arrows) and petechial hemorrhage in the left temporal lobe. **(C)** TFCA confirms Borden grade 3 AVF, with feeders from the left occipital artery and middle meningeal artery draining into the transverse sinus.

AVF = arteriovenous fistula, m-SWI = multi-echo SWI, s-SWI = single-echo SWI, SWI = susceptibility-weighted image, TFCA = transfemoral cerebral angiography

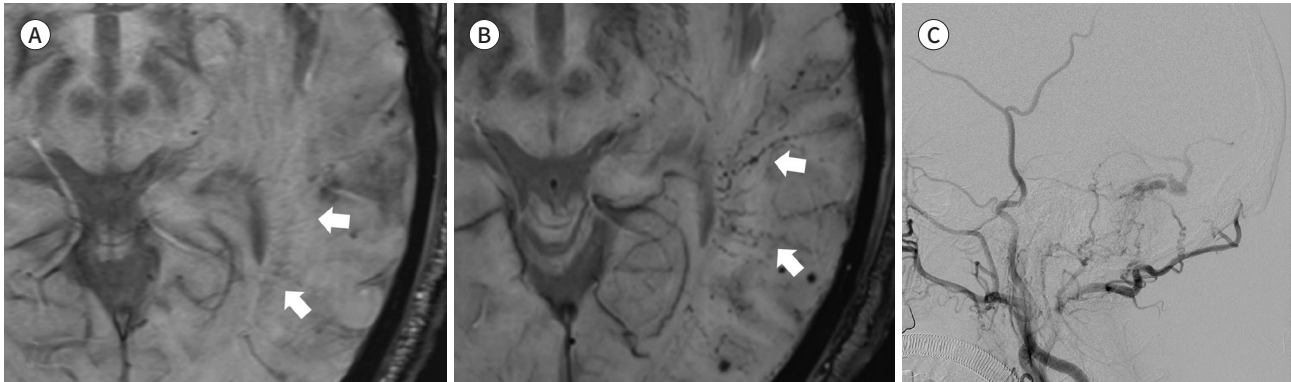


Table 4. Interobserver Agreement for T2WI and SWI (n = 28)

Parameters	Kappa Value	95% CI
T2WI	0.42 (moderate)	0.06–0.78
SWI	0.51 (moderate)	0.10–0.92
Image quality	0.48 (moderate)	0.20–0.75

Interobserver agreement among two readers of MR pulse sequences (T2WI and SWI) was calculated utilizing unweighted Cohen's Kappa, while linear-weighted Cohen's Kappa was calculated for image quality evaluation.

CI = confidence interval, SWI = susceptibility weighted image, T2WI = T2-weighted image

detection of AVM than AVF due to good visualization of prominent conglomerated flow-voids at the AVM nidus and draining vein dilatation.

In the qualitative evaluation of SWI image quality, 14/28 (50.0%) SWI images were categorized as good, 9/28 (32.1%) were average, and 5/28 (17.9%) were poor. Specifically, m-SWI demonstrated better image quality than s-SWI (poor: 8.3% vs. 25.0%; average: 8.3% vs. 50.0%; good: 83.3% vs. 25.0%, $p = 0.009$) (Table 3). Compared to s-SWI, m-SWI demonstrated much more conspicuity of the dilated small veins for AVF and clear demarcation of the AVM nidus (Figs. 4, 5). The 5 cases of poorly visualized vascular lesions on SWI included 2 AVF on s-SWI, 1 AVF on m-SWI, and 2 CCFs on s-SWI. The two poorly visualized AVFs on s-SWI were Borden classification 3 in the left temporal lobe, with main feeders from the left external carotid arteries, draining into the cortical veins. The poorly visualized AVF on m-SWI was Borden classification 1 in the left cerebellum, feeders from the ipsilateral occipital artery, and draining into the sigmoid sinus. The two poorly visualized cases of CCF on s-SWI had fistulas in the left cavernous sinuses with Barrow classification A + C, and Barrow classification C. For both CCF cases, the left cavernous sinuses did not have asymmetric distensions or high signal intensity,

despite direct high-flow feeder from the ipsilateral internal carotid artery for Barrow classification A + C.

The interobserver agreements between the two readers were as follows: moderate for T2WI evaluation ($\kappa = 0.42$, 95% CI: 0.06–0.78), moderate for SWI ($\kappa = 0.51$, 95% CI: 0.10–0.92), and moderate for image quality evaluation ($\kappa = 0.48$, 95% CI: 0.20–0.75) (Table 4).

DISCUSSION

Cerebral arteriovenous shunts are rare and difficult to diagnose due to various neurological symptoms (1-3, 8, 24). One of the useful, non-invasive imaging modalities in diagnosing the arteriovenous shunts is the SWI, which demonstrated a superb diagnostic performance in detecting AVM with intracerebral hemorrhage and post-treated AVM, and demonstrated its utility in evaluating the draining veins of AVM and post-radiosurgery status of AVM (13, 14, 25). In our study, we compared sensitivity of non-contrast enhanced MR pulse sequences, T2WI and SWI for detecting vascular lesions. The overall SWI sensitivity was higher than T2WI (82.1% vs. 53.6%, $p = 0.013$) with moderate interobserver agreement ($\kappa = 0.51$).

A comparative qualitative evaluation of s-SWI and m-SWI was performed, with m-SWI demonstrating better image quality in characterizing vascular lesions (good quality: 83.3% vs. 25.0%, $p = 0.009$) with moderate agreement ($\kappa = 0.48$). Additional data may demonstrate the superiority of m-SWI compared with s-SWI in the detection of various cerebral arteriovenous shunts, based on our finding that only 1 of 12 vascular lesions was poorly visualized using m-SWI. Our findings also imply that physicians may benefit from m-SWI in the early detection or screening of cerebral arteriovenous shunts due to its rapid image acquisition time, the convenience of not requiring contrast media, and good image quality in characterizing vascular lesions.

SWI takes advantage of concentrations in oxygenated and deoxygenated hemoglobin concentration in the vessels; specifically, slow-flowing veins normally have low signal intensity, while fast-flowing arteries with high concentration of oxyhemoglobin demonstrate high signal intensity, thus functioning as flow-related enhancement (7, 16, 26). As our results demonstrated, SWI was able to sensitively detect cerebral arteriovenous shunts better than T2WI, owing to its better delineation of arterialized veins and sinuses, and its ability to delineate the asymmetrically dilated small veins. In addition, moderate interobserver agreements of SWI and image qualities of SWI implied good readability and consistency of SWI in terms of detecting the vascular lesions. Conversely, the relatively poor performance of T2WI in the detection of cerebral arteriovenous shunts is due to the lack of flow-related enhancement and its limitations in detecting small, dilated veins and petechial hemorrhages. One limitation of m-SWI is that if echoes are partially flow compensated in the readout direction, they may cause signal loss, delineating fast-flowing arteries as veins (18, 27). The other limitations of SWI may include artifact at the skull base, poor evaluation of hemodynamics, and underestimation of AVM nidus size, and Spetzler-Martin grade, thereof.

Compared with conventional s-SWI, m-SWI is known to have better image quality with higher signal-to-noise ratio and contrast-to-noise ratio. A previous study reported that combined m-SWI and phase filter images increased the signal-to-noise ratio by approximately 46%

and increased contrast-to-noise ratio by 34% to 80%, compared with single-echo SWI (18). Similarly, multi-echo gradient echo sequence demonstrated higher contrast-to-noise ratio and superior image quality compared with TOF angiography; specifically, venous structures, such as internal cerebral veins, were visualized by the multi-echo gradient echo sequence, otherwise poorly visualized on TOF angiography (17). Similarly, in our study, the improvement of image quality of m-SWI rendered better visibility and readability of cerebral arteriovenous shunts than conventional s-SWI and T2WI. After the qualitative evaluation, m-SWI demonstrated conspicuity in delineating asymmetrically dilated small veins in AVF (Fig. 5). In addition, m-SWI demonstrated visualization of high signals at the arterialized veins and sinuses in AVF, and visualization of nidus formation, even for distally located AVM (Fig. 4).

Similar to SWI, arterial spin labeling (ASL) is another non-invasive MR protocol, which can effectively visualize cerebral arteriovenous shunting, when utilized as an adjunct to conventional MR protocols (28). ASL is known for depicting signals within venous structures of arteriovenous shunts, which makes it useful for sensitively detecting high-flowing AVF or malformation. However, compared to the SWI magnitude image, ASL takes longer time for image acquisition time (approximately 5–6 minutes), and it may display lower image quality with decreased anatomical correlation, not to mention MR artifacts during magnetic labeling process (28, 29). In addition, ASL may demonstrate lower sensitivity than SWI for low-flowing arteriovenous shunts such as AVM with small nidus and dural AVF with small volume of shunting blood (28, 30). On the other hand, SWI may be sensitive in depicting small, dilated vessels and abnormally dilated vessels regardless hemodynamics of the cerebral arteriovenous shunts, unless located near the skull base.

Our study had several limitations. The first was the small sample size and different MR parameters used by three MR vendors, which may limit the generalizability of our findings. Our study intention was to evaluate preliminarily how non-contrast enhanced sequences such as T2WI and SWI delineated various cerebral arteriovenous shunts, and how SWI performed in detecting the vascular lesions. Despite the small sample sizes, statistical significance in sensitivity of SWI and qualitative evaluation of both SWI modalities was demonstrated. m-SWI's excellent visibility and good image quality of delineation of such vascular lesion may provide many advantages to clinicians and radiologists in the out-patient settings, and may provide good foundations for the future study. We speculate that additional data will strengthen our findings regarding consistency of the ability m-SWI to detect small vein dilatations in AVF, AVM with a small nidus, and distally located AVM. Second, owing to the retrospective nature of the study, selection bias and recall bias may have been introduced during the evaluation. However, we attempted to minimize bias by randomization of T2WI, SWI images after blinding the TFCA findings and clinical information. Third, we did not include 1:1 matched normal control group to evaluate the specificity and accuracy of T2WI and SWI.

In conclusion, SWI demonstrated higher sensitivity in detecting cerebral arteriovenous shunts (AVF, AVM, CCF) than conventional T2WI. In terms of characterizing vascular lesion, m-SWI demonstrated better image quality than s-SWI.

Author Contributions

Conceptualization, H.S.W., S.J.H.; data curation, all authors; formal analysis, all authors; investigation, all authors; methodology, all authors; project administration, S.J.H.; supervision, S.J.H.; valida-

tion, all authors; visualization, all authors; writing—original draft, H.S.W., S.J.H.; and writing—review & editing, all authors.

Conflicts of Interest

The authors have no potential conflicts of interest to disclose.

Funding

None

REFERENCES

1. Abecassis IJ, Xu DS, Batjer HH, Bendok BR. Natural history of brain arteriovenous malformations: a systematic review. *Neurosurg Focus* 2014;37:E7
2. Gandhi D, Chen J, Pearl M, Huang J, Gemmete JJ, Kathuria S. Intracranial dural arteriovenous fistulas: classification, imaging findings, and treatment. *AJNR Am J Neuroradiol* 2012;33:1007-1013
3. Reynolds MR, Lanzino G, Zipfel GJ. Intracranial dural arteriovenous fistulae. *Stroke* 2017;48:1424-1431
4. Ellis JA, Goldstein H, Connolly ES Jr, Meyers PM. Carotid-cavernous fistulas. *Neurosurg Focus* 2012;32:E9
5. Hillman J. Population-based analysis of arteriovenous malformation treatment. *J Neurosurg* 2001;95:633-637
6. Chen CJ, Ding D, Derdeyn CP, Lanzino G, Friedlander RM, Southerland AM, et al. Brain arteriovenous malformations: a review of natural history, pathobiology, and interventions. *Neurology* 2020;95:917-927
7. Hodel J, Leclerc X, Kalsoum E, Zuber M, Tamazyan R, Benadjaoud MA, et al. Intracranial arteriovenous shunting: detection with arterial spin-labeling and susceptibility-weighted imaging combined. *AJNR Am J Neuroradiol* 2017;38:71-76
8. Ozpinar A, Mendez G, Abla AA. Epidemiology, genetics, pathophysiology, and prognostic classifications of cerebral arteriovenous malformations. *Handb Clin Neurol* 2017;143:5-13
9. Gross BA, Frerichs KU, Du R. Sensitivity of CT angiography, T2-weighted MRI, and magnetic resonance angiography in detecting cerebral arteriovenous malformations and associated aneurysms. *J Clin Neurosci* 2012;19:1093-1095
10. Essig M, Wenz F, Schoenberg SO, Debus J, Knopp MV, Van Kaick G. Arteriovenous malformations: assessment of gliotic and ischemic changes with fluid-attenuated inversion-recovery MRI. *Invest Radiol* 2000;35:689-694
11. Kwon BJ, Han MH, Kang HS, Chang KH. MR imaging findings of intracranial dural arteriovenous fistulas: relations with venous drainage patterns. *AJNR Am J Neuroradiol* 2005;26:2500-2507
12. Schneider TM, Möhlenbruch M, Denoix M, Ladd ME, Bendszus M, Heiland S, et al. Susceptibility-based characterization of cerebral arteriovenous malformations. *Invest Radiol* 2020;55:702-710
13. Finitis S, Anxionnat R, Gory B, Planel S, Liao L, Bracard S. Susceptibility-weighted angiography for the follow-up of brain arteriovenous malformations treated with stereotactic radiosurgery. *AJNR Am J Neuroradiol* 2019;40:792-797
14. Jagadeesan BD, Delgado Almandoz JE, Moran CJ, Benzinger TL. Accuracy of susceptibility-weighted imaging for the detection of arteriovenous shunting in vascular malformations of the brain. *Stroke* 2011;42:87-92
15. Heit JJ, Thakur NH, Iv M, Fischbein NJ, Wintermark M, Dodd RL, et al. Arterial-spin labeling MRI identifies residual cerebral arteriovenous malformation following stereotactic radiosurgery treatment. *J Neuroradiol* 2020;47:13-19
16. Radbruch A, Mucke J, Schweser F, Deistung A, Ringleb PA, Ziener CH, et al. Comparison of susceptibility weighted imaging and TOF-angiography for the detection of Thrombi in acute stroke. *PLoS One* 2013;8:e63459
17. Boeckh-Behrens T, Lutz J, Lummel N, Burke M, Wesemann T, Schöpf V, et al. Susceptibility-weighted angiography (SWAN) of cerebral veins and arteries compared to TOF-MRA. *Eur J Radiol* 2012;81:1238-1245
18. Denk C, Rauscher A. Susceptibility weighted imaging with multiple echoes. *J Magn Reson Imaging* 2010;31:185-191
19. Barrow DL, Spector RH, Braun IF, Landman JA, Tindall SC, Tindall GT. Classification and treatment of spontaneous carotid-cavernous sinus fistulas. *J Neurosurg* 1985;62:248-256

20. Spetzler RF, Martin NA. A proposed grading system for arteriovenous malformations. *J Neurosurg* 1986;65:476-483
21. Kim D, Choi YJ, Song Y, Chung SR, Baek JH, Lee JH. Thin-section MR imaging for carotid cavernous fistula. *AJNR Am J Neuroradiol* 2020;41:1599-1605
22. Wen HY, Chen HC, Yang ST. Risk factors of aggressive clinical presentation in patients with angiographically aggressive cranial dural arteriovenous fistulas. *J Clin Med* 2021;10:5835
23. Viera AJ, Garrett JM. Understanding interobserver agreement: the kappa statistic. *Fam Med* 2005;37:360-363
24. Miller TR, Gandhi D. Intracranial dural arteriovenous fistulae: clinical presentation and management strategies. *Stroke* 2015;46:2017-2025
25. Miyasaka T, Taoka T, Nakagawa H, Wada T, Takayama K, Myochin K, et al. Application of susceptibility weighted imaging (SWI) for evaluation of draining veins of arteriovenous malformation: utility of magnitude images. *Neuroradiology* 2012;54:1221-1227
26. Gasparotti R, Pinelli L, Liserre R. New MR sequences in daily practice: susceptibility weighted imaging. A pictorial essay. *Insights Imaging* 2011;2:335-347
27. Deistung A, Dittrich E, Sedlacik J, Rauscher A, Reichenbach JR. ToF-SWI: simultaneous time of flight and fully flow compensated susceptibility weighted imaging. *J Magn Reson Imaging* 2009;29:1478-1484
28. Amukotuwa SA, Yu C, Zaharchuk G. 3D pseudocontinuous arterial spin labeling in routine clinical practice: a review of clinically significant artifacts. *J Magn Reson Imaging* 2016;43:11-27
29. Lindner T, Jansen O, Helle M. Time-resolved high-resolution angiography combining arterial spin labeling and time-of-flight imaging. *Appl Magn Reson* 2020;52:201-210
30. Amukotuwa SA, Marks MP, Zaharchuk G, Calamante F, Bammer R, Fischbein N. Arterial spin-labeling improves detection of intracranial dural arteriovenous fistulas with MRI. *AJNR Am J Neuroradiol* 2018;39:669-677

뇌동정맥단락 진단에서의 단일 에코 자화율 강조영상과 다중 에코 자화율 강조영상의 비교: 예비 연구

한승완¹ · 신재호^{1*} · 인연권¹ · 양승호² · 성재훈²

목적 뇌동정맥루(arteriovenous fistula; 이하 AVF), 뇌동정맥기형(arteriovenous malformation; 이하 AVM), 경동맥해면정맥동루(carotid-cavernous sinus fistula; 이하 CCF) 등 뇌동정맥단락을 진단하는 데 있어서, T2 강조영상(T2-weighted imaging; 이하 T2WI)과 자화율 강조영상(susceptibility-weighted imaging; 이하 SWI)의 민감도를 비교하고, 단일 에코(single-echo) SWI(이하 s-SWI)와 다중 에코(multi-echo) SWI(이하 m-SWI)의 전반적인 영상 질을 비교하고자 하였다.

대상과 방법 2016년부터 2021년까지 뇌혈관조영술로 입증된 뇌동정맥단락을 조사하였다. 뇌동정맥단락에 대한 T2WI와 SWI의 민감도를 McNemar's Test를 이용하여 비교하였다. s-SWI와 m-SWI의 영상 질을 나쁨, 보통, 좋음으로 분류하고 Fisher's exact test를 이용하여 그 비율을 비교하였다.

결과 총 24명의 환자(중위 연령: 61세, 여성: 12명, 남성: 12명)가 연구에 포함되었다. 그중 4명은 s-SWI와 m-SWI 두 가지의 SWI로, 나머지 20명은 이 중 한 가지의 SWI로 검사하였다. 10명은 AVF, 11명은 AVM, 3명은 CCF로 진단되었고, 이와 같은 뇌동정맥단락에 대해, SWI는 T2WI 보다 유의하게 높은 민감도를 보였다(82.1% vs. 53.6%, $p = 0.013$). m-SWI는 s-SWI 보다 좋은 영상 질의 비율이 유의하게 높았다(83.3% vs. 25.0%, $p = 0.009$).

결론 SWI는 T2WI 보다 뇌동정맥단락을 더 민감하게 진단해 낼 수 있었으며, m-SWI는 s-SWI보다 혈관질환을 평가하는데 더 좋은 영상 질을 보였다.

가톨릭대학교 의과대학 성빈센트병원 ¹영상의학과, ²신경외과